Desalination and Water Treatment
www.deswater.com
1944-3994/1944-3986 © 2013 Desalination Publications. All rights reserved
doi: 10.1080/19443994.2012.714526

51 (2013) 476–484
January

Taylor & Francis
Taylor & Francis Group

Using nanofiltration in a "zero-rejection" process: the removal of Ni^{2+} and Co^{2+} from salty wastewater

Caue Ferreira Esmi[a], Luc Schrive[a,*], Yves Barre[a], John Palmeri[b], Andre Deratani[c]

[a]*CEA, DEN, DTCD/SPDE/LPSD—Marcoule, F-30207, Bagnols-sur-Cèze, France*
Tel. +33 466339472; email: luc.schrive@cea.fr
[b]*Université Paul Sabatier—Toulouse III, CNRS (IRSAMC), 31062 Toulouse Cedex 4, France*
[c]*Institut Européen des Membranes, Université Montpellier 2, 34095 Montpellier cedex 05, France*

Received 2 March 2012; Accepted 18 July 2012

ABSTRACT

The use of nanofiltration as a pretreatment step in a zero rejection process was investigated. Nanoflux, a nanofiltration simulation software, was used to predict the rejection of Co^{2+} and Ni^{2+} from a salty multi-element matrix whose concentration is similar to seawater. Orientation simulations prior to filtration experiments were made with Nanoflux® in order to predict ionic rejections. Previously, the multi-element matrix solution speciation was studied by JChess. It was shown that the effective membrane charge and the effective membrane thickness, adjusted through the filtration of a single salt $NaNO_3$ solution, could be used to predict the ionic rejections of the multi-element solution for two commercial nanofiltration membranes. The elevated concentration of $NaNO_3$ in the multi-electrolyte solution did not reduce the high ionic selectivity of divalent ions. Predicted values were in good agreement with experimental results at neutral pH of the multi-electrolyte solution.

Keywords: Nanofiltration; Wastewater; Zero-rejection; Heavy metals

1. Introduction

Water pollution generated by heavy metal wastewater discharge is an environmental problem created by industries such as mining, surface treatment and paper industries. In this context, new environmentally friendly processes, based on the concept of zero-rejection, have drawn a lot of attention in recent years. Within such processes no toxic substances would be released to the environment [1].

Currently, chemical precipitation is widely used to treat industrial wastewater mainly due to its convenient operation and economical cost. However, the final concentration of the treated solution may be insufficient to fulfill the strict environmental regulations. In these cases, complementary treatments such as ion exchange resins are used. Despite the advantages of such an approach, the considerable amount of acidic secondary waste produced for resin regeneration constitutes an important limitation to the process [2].

A new technique specially designed for treating heavy metals in aqueous solutions was recently described [3]. It uses a chelating polymer-modified electrode to remove heavy metals present at low concentration levels. A localized acidic medium generated by water electrolysis at the polymer-solution

*Corresponding author.

Presented at the International Conference on Desalination for the Environment, Clean Water and Energy, European Desalination Society, 23–26 April 2012, Barcelona, Spain

interface regenerates the system. The amount of H^+ produced is not enough to alter the pH of the global solution so no acidic secondary waste is produced. Although advantageous, this Electrochemical Controlled (EC) ion complexation technique, in its current state of development, cannot be efficiently used as a sole technique to treat solutions whose concentration exceeds a few dozens of mg/l. The association of nanofiltration—a cross-flow membrane separation technique known for its high removal of divalent ions—as a pre-treatment step to EC technique would enable us to create a process suitable for removing heavy metal in wastewaters following the zero-reject concept.

The low concentration filtrate issuing from nanofiltration would be used by EC to produce a potentially treated stream. No secondary effluents would be produced by EC, as the concentrated eluted flow would be sent back to nanofiltration. Nanofiltration brine could then be treated by a final classical technique.

Since the overall process performance is limited by the capacity of the chelating polymers in the EC step, it is important to predict heavy metals nanofiltration rejections in the pretreatment step.

First, we demonstrate how the use of JChess chemical speciation software and Nanoflux® allowed us to perform nanofiltration experiments in optimal conditions. We then explain how two sets of adjustable parameters—membrane charge (X_m) and effective membrane thickness (L_{eff})—obtained on the filtration of a simpler $NaNO_3$ solution can be used to predict ionic rejection of the multi-element solution.

2. Materials and methods

It is well known that, in nanofiltration, ionic rejections depend on the solution composition (concentration, pH), process parameters (transmembrane pressure [TMP]), and membrane/solution interactions. Experimentally studying all factors affecting rejection by nanofiltration in such a complex solution (Table 1) would require numerous experiments. The use of Nanoflux® to predict Co^{2+} and Ni^{2+} rejections will be time saving. Thus, we evaluate the filtration performance of two commercial nanofiltration membranes using the Nanoflux® database and analyze the suitability of the nanofiltration step in the zero-rejection process.

Table 1
Composition of the multi-electrolyte solution studied

Composition	Concentration (M)
$Co(NO_3)_2$	6.4×10^{-3}
$Ni(NO_3)_2$	3.4×10^{-5}
$NaNO_3$	0.6
$NaNO_2$	2.0×10^{-2}
Na_2SO_4	2.0×10^{-2}

2.1. Membranes

Two different organic nanofiltration membranes were experimentally studied, Desal-5DK and Desal-5DL (GE-Osmonics). Before utilization, each membrane was tested through the filtration of a simple synthetic $MgSO_4$ solution. Mg^{2+} and SO_4^{2-} ionic concentrations were measured by a conductivity meter. Ionic rejections, calculated by Eq. (1), were more than 98%.

$$R(\%) = 100\left(1 - \frac{c_i^p}{c_i^f}\right) \quad (1)$$

where, c_i^p is the ionic concentration of species i in the permeate in mol l^{-1} and c_i^f is the ionic concentration of species i in the feed in mol l^{-1}.

2.2. Experimental

Experiments were carried out on a SEPA CF II (GE Water & Process) set up, equipped with one shim piece of 25 mil (0.64 mm) and one feed spacer of 31 mil (0.79 mm). In such a system, membrane active area is 138 cm^2. Feed solution was pumped at a constant rate of 250 l/h. TMP was adjusted. Permeate solution was fully recycled to the feed solution, maintaining a constant salt concentration. Temperature of the feed solution was regulated at 25.0 ± 0.2 °C. All reagents used to prepare synthetic solutions were supplied from Sigma-Aldrich (ACS reagent grade).

Prior to each filtration experiment, the pure water hydraulic permeability, L_p^0 ($1\,h^{-1}\,m^{-2}\,bar^{-1}$), was measured. Pure water (15 MΩ) was used. Average values for Desal-5DL and Desal-5DK membranes are 5.5 and $7.8\,l\,h^{-1}\,m^{-2}\,bar^{-1}$, respectively.

When performing $NaNO_3$ filtration experiments, the pH of the feed solution was not altered and measured to be 5.8. Rejections of Na^+ and NO_3^- were considered to be equivalent. Solution conductivity was then measured and ionic concentrations were obtained through a calibration curve.

Experiments on the multi-electrolyte solution were carried out at two different pH values for each

membrane: the non modified value of approximately 6.5 and an acid value of approximately 3. Concentrations of Na^+, NO_3^-, SO_4^{2-}, and NO_2^- were measured by ionic chromatography. Ni^{2+} and Co^{2+} concentrations were determined by ICP-MS.

3. Nanofiltration ion transport model

A theoretical prevision for ionic rejections of multi electrolyte solutions can be provided by the hindered electro-transport (HET) theory which uses the Extended Nernst–Planck (ENP) equation and volume averaged Stokes equation to describe ionic and solution flux through the membrane [4]. Equations are provided in the Appendix.

HET theory considers that the ionic partition at the solution/membrane interface is only produced by steric and Donnan effects. Dielectric effects were later added to the theory, leading to an extended hindered electrotransport (EHET) theory. These three effects are integrated into an ionic partition coefficient (k_i) that may be written as the product of each individual effect as shown by Eq. (2) and Table 2 [5]:

$$k_i^{f(p)} = \frac{\overline{c}_i^{f(p)}}{c_i^{f(p)}} = k_{i,\text{steric}} \cdot k_{i,\text{Donnan}} \cdot k_{i,\text{dielectric}} \quad (2)$$

In this work, simulated ionic rejections are calculated by Nanoflux® using a modified EHET theory [6,7]. ENP equation and volume averaged Stokes equation are numerically solved using the software internal database—containing values of Pauling radius, ionic charge, and bulk diffusion coefficients—and a set of user adjustable input parameters:

c_i^f: the ionic concentration in the feed in mol l^{-1},
X_m: corresponding to the effective membrane charge density in mol l^{-1},
r_p: the membrane pore radius,
L_{eff}: the effective membrane thickness in μm, $L_{eff} = l_m(\frac{\varphi}{\tau})$,
L_p^0: the pure water hydraulic permeability (L/(h m^2 bar)).

The use of Pauling radius instead of stokes radius is based on studies from ion transport in biological channels and is justified in references [6,8]. As Nanoflux® does not consider the dielectric effects, its contribution to the partition coefficients must be manually calculated and entered in the form of a residual coefficient ($k_{i,\text{residual}}$). Such dielectric effects were extensively studied in references [9,10]. Although being composed of the Born effect ($\Delta W_{i,\text{Born}}$)—related to the difference between the dielectric constant of the solvent in the bulk solution and inside the membrane pores—and an image charge effect ($\Delta W_{i,\text{im}}$)—related to the difference in the dielectric constant of the solvent and the membrane—, our calculations assumed that dielectric exclusion and thus $k_{i,\text{residual}}$ is only made up by the Born effect (see Appendix). Such an assumption is based on the difficulty of setting a correct value for the membrane dielectric constant [11].

4. Results and discussion

4.1. pH values to filtration experiences

Altering the solution pH can substantially change the speciation of the solution. For example, metal precipitates could be formed at higher pH values. Nanofiltration membranes, due to its reduced pore radius, are especially sensitive to fouling. In order to know from which pH values precipitates might be formed, JChess, a chemical speciation software, was used to calculate the multi-electrolyte speciation. The main species concentration as a function of solution pH is shown in Fig. 1.

Species present in the solution include not only the expected Co^{2+}, Ni^{2+}, SO_4^{2-}, NO_3^-, NO_2^-, and Na^+, but also minority ones such as $CoNO_3^-$ and $NaSO_4^-$. At pH values lower than 4.6, $HNO_{2(aq)}$ is also formed. For pH values higher than 7, Co^{2+} concentration decreases as the precipitate $CoCO_3$ is formed. CO_3^{2-} is added to feed solution by atmospheric CO_2 dissolution. Such precipitation would be hardly noticed without the use of JCHESS. In order to avoid the formation of precipitates in solution, no filtration experiments were made at pH

Table 2
Components of partition coefficient

Effect	Coefficient	Equation
Steric exclusion	$k_{i,\text{steric}}$	$k_{i,\text{steric}} = \left(1 - \frac{r_i}{r_p}\right)^2$
Donnan exclusion	$k_{i,\text{Donnan}}$	$k_{i,\text{Donnan}} = \exp(-\frac{z_i F}{RT}\Delta\psi_D)$
Dielectric exclusion	$k_{i,\text{dielectric}}$	$k_{i,\text{dielectric}} = \exp(-\Delta W_{i,\text{Born}})\exp(-\Delta W_{i,\text{im}})$

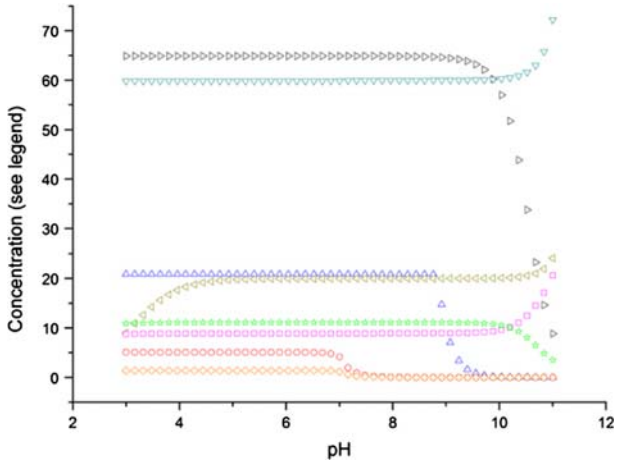

Fig. 1. Multi-electrolyte solution speciation as a function of the pH. JCHESS calculations data: ○ Co^{2+} (mmolal), △ Ni^{2+} (μmolal), □ SO_4^{2-} (mmolal), ▽ NO_3^- (x10mmolal), ◁ NO_2^- (mmolal) and ▷ Na^+ (x10mmolal), ☆ $NaSO_4^-$ (mmolal), ◇ $CoNO_3^-$ (mmolal).

values higher than the natural solution pH (6.5) where no precipitation occurs.

Moreover, nanofiltration membranes, for a certain pH value known as isoelectric point (IEP), carry no net electrical charge [12]. In such conditions ion rejection greatly decreases as it will be only due to steric retention. Using r_p and L_p^0 values from Nanoflux® membrane database, one is able to determinate IEP of Desal-5DL and Desal-5DK before any filtration experiment. By entering the multi-electrolyte solution composition, the software is able to calculate suggested X_m and L_{eff} values. Details are presented in [8]. These two parameters, even if not yet totally adjusted to the system, may be used to simulate ionic rejections as a function of pH (Fig. 2).

A clear IEP is not noticeable for both membranes, even though an increase in ionic rejection is observed with increasing pH for the Desal-5DK membrane. Desal-5DL membrane, apart from the SO_4^{2-} ion, presents a stable ionic rejection in the range of the pH studied. Membrane charge can be seen as the sum of two different contributions, a proper charge, caused by acid/base dissociation of functional sites at the membrane surface and a charge, caused by ionic adsorption [13]. In the multi-electrolyte solution, the elevated concentration of Na^+ and NO_3^- could make the adsorption charge contribution to be much more significant than proper charge, which is more dependent on pH.

Considering that Desal-5DL and Desal-5DK membranes can be used in pH values up to 2 and aiming to experimentally evaluate the effect of pH in ionic rejection of both membranes, we decided to perform the multi-electrolyte solution filtration experiments in the natural solution pH and in an acidic value of 3.

4.2. Ion rejection predictions

Among the parameters used by Nanoflux® to calculate ionic rejections, X_m and L_{eff} are those more closely related to the feed solution. The more accurate these two parameters are, the better the prevision made by the model is. Nanoflux® proposes a fitting procedure in which X_m and L_{eff} values will be adjusted in order to minimize mean square deviation between experimental and calculated points

As the main objective of this work is to use Nanoflux® as a predictive tool, adjusting calculated ionic rejections of the multi-electrolyte solution to experimental values in order to achieve a good prevision

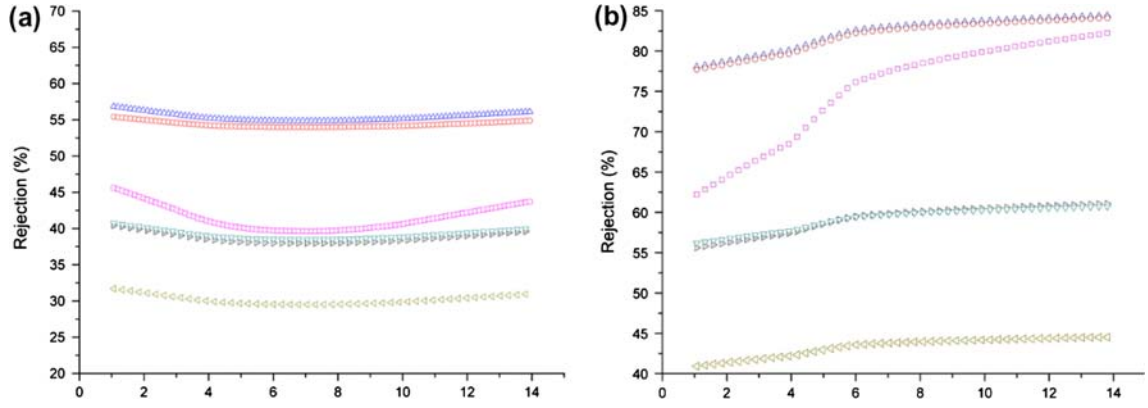

Fig. 2. Ionic rejection values as a function of pH at 21 bar and 25°C. ○ Co^{2+}, △ Ni^{2+}, □ SO_4^{2-}, ▽ NO_3^-, ◁ NO_2^- and ▷ Na^+. (a) Desal-5DL membrane, r_p 0.58 nm, L_p^0 5.9 (L/(h m² bar)). (b) Desal-5DK membrane, r_p 0.44 nm, and L_p^0 7.6 (L/(h m² bar)).

would be senseless. Moreover, as different operating parameters may result on different system behaviors, this approach could quickly result on numerous experiments.

Considering that almost 96% of the multi-electrolyte solution is composed of $NaNO_3$ salt, easily measured by a conductivity meter, we propose that X_m and L_{eff} values obtained from the fit to experimental Na^+ and NO_3^- rejections could be used to calculate the multi-electrolyte solution ionic rejections.

Proceeding in this way, we obtained fitted values of X_m and L_{eff} were −0.53 mol/L and 0.426 μm for the Desal-5DL membrane and −0.05 mol/L and 0.374 μm for the Desal-5DK membrane. These values were then used in the multi-electrolyte ionic rejections calculations.

4.2.1. Natural pH

The multi-electrolyte solution at its natural pH of 6.4 was filtered by Desal-5DK and Desal-5DL membranes. Once the experimental ionic rejections of the multi-electrolyte solution were obtained, a fit process was done in order to obtain the values of X_m and L_{eff} that would be used by the HET theory in the best accurate ionic rejections simulations.

For the Desal-5DK and Desal-5DL membranes, Fig. 3 and in Fig. 4 present, respectively, experimental and simulated ionic rejection values using X_m and L_{eff} from (a) $NaNO_3$ fit and (b) multi-electrolyte solution fit.

Experimental ionic rejection rates for both membranes are typical of nanofiltration. Higher values were obtained for divalent ions than for monovalent ones, confirming the high selectivity of the technique

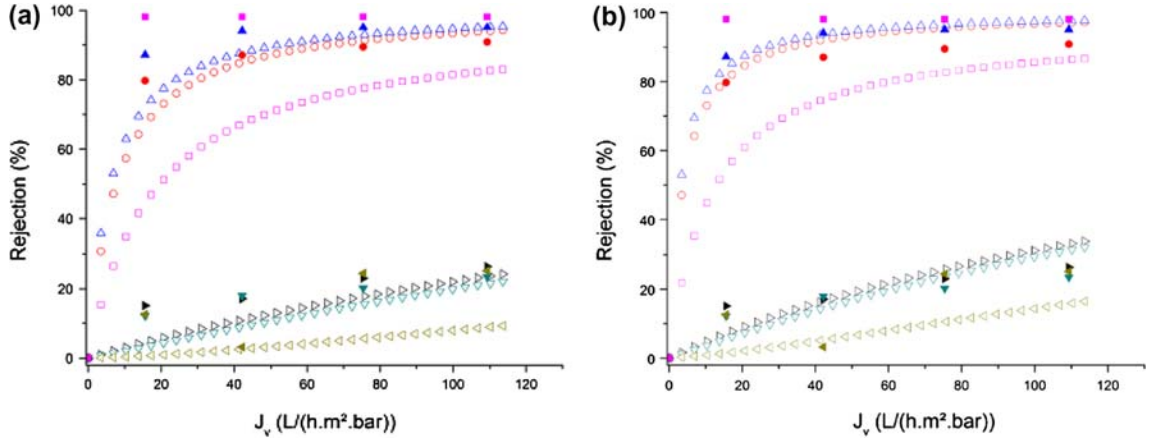

Fig. 3. Nanoflux® ionic rejection simulation/experimental data for the Desal-5DK membrane: ○/● Co^{2+}, △/▲ Ni^{2+}, □/■ SO_4^{2-}, ▽/▼ NO_3^-, ◁/◀ NO_2^- and ▷/▶ Na^+. pH = 6.4. (a) $NaNO_3$ fit and (b) multi-electrolyte solution fit.

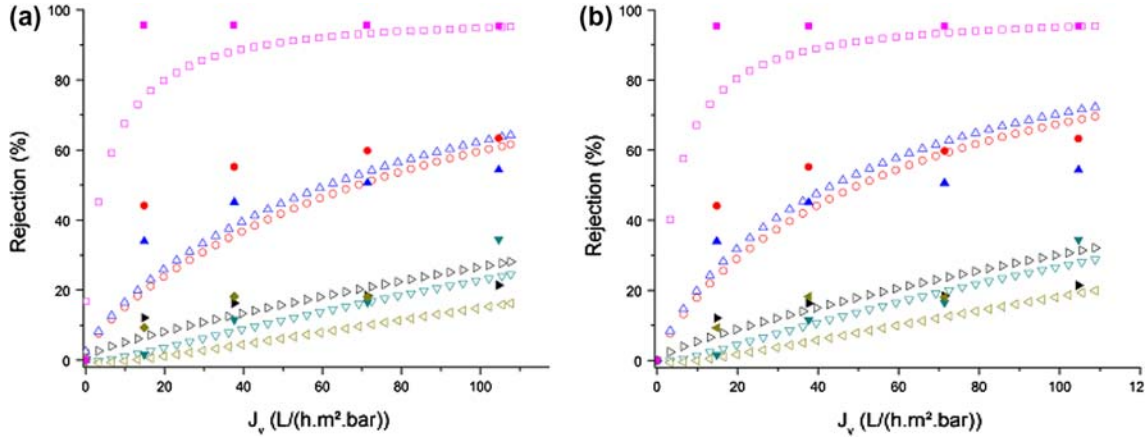

Fig. 4. Nanoflux® ionic rejection simulation/experimental data for the Desal-5DL membrane: ○/● Co^{2+}, △/▲ Ni^{2+}, □/■ SO_4^{2-}, ▽/▼ NO_3^-, ◁/◀ NO_2^- and ▷/▶ Na^+. pH = 6.4. (a) $NaNO_3$ fit and (b) multi-electrolyte solution fit.

Table 3
Best fit values of X_m and L_{eff} for the Desal-5DL and Desal-5DK membranes at natural pH—modified EHET theory

	$NaNO_3$		Multi-electrolyte solution	
Membrane	X_m (mol l^{-1})	L_{eff} (μm)	X_m (mol l^{-1})	L_{eff} (μm)
Desal-5DL	−0.53	0.426	−0.47	0.749
Desal-5DK	−0.05	0.374	−0.04	0.661

in a multi/monovalent ion separation. Nanoflux® simulations for both membranes were able to simulate such behavior. Moreover, simulated rejections using adjusted parameters from the $NaNO_3$ single salt solution were in good agreement with those from the multi-electrolyte solution. When comparing the two membranes, Co^{2+} and Ni^{2+} rejections are better predicted for the Desal-5DK membrane. However for this membrane, SO_4^{2-} rejection is underestimated. Table 3 compares X_m and L_{eff} obtained from the two fitting procedures.

For both membranes, adjusted values of X_m from the $NaNO_3$ solution are close to the ones from the multi-electrolyte solution. However, L_{eff} values are almost two times smaller.

It should be noted that using the fitting procedure for obtaining X_m and L_{eff} tries to compensate for effects that are not taken into account when Nanoflux® uses the HET theory. Better ionic rejections simulations would be obtained if one considered, for example, the speciation of the solution as presented in Fig. 1 and the image charge effects from the partition coefficients. Considering the solution complexity, a standard deviation value of 2.4% between $NaNO_3$ solution fitted simulations and experimental results for both membranes reveals a reasonably good prediction from the model.

Table 4
Ionic rejections at TMP of 22 bar, natural pH

Ion	Desal-5DK rejection (%)	Desal-5DL rejection (%)
Na^+	26	21
Ni^{2+}	>95	54
Co^{2+}	90	63
NO_3^-	23	34
NO_2^-	25	18[a]
SO_4^{2-}	>98	>95

[a]Measured at 16 bar.

Comparison between Desal-5DL and Desal-5DK membranes reveals similar experimental ionic rejection values of approximately 20% (Table 4) for monovalent ions. However, rejection of divalent ions is higher for Desal-5DK (approximately 90%) than for Desal-5DL membrane (approximately 60%). Such a fact cannot be entirely explained by an increasing steric exclusion caused by the smaller pore radius of the Desal-5DK membrane. NO_3^-, for example, has a similar ionic radius to Ni^{2+} and

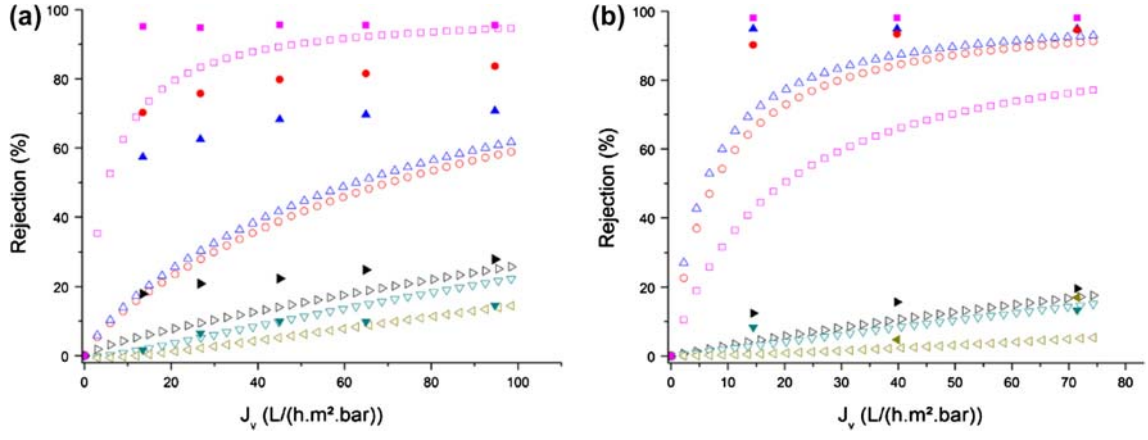

Fig. 5. Nanoflux® ionic rejection calculation/experimental data: ○/● Co^{2+}, △/▲ Ni^{2+}, □/■ SO_4^{2-}, ▽/▼ NO_3^-, ◁/◀ NO_2^- and ▷/▶ Na^+. pH = 3.2. (a) Desal-5DL and (b) Desal-5DK.

Table 5
Cation rejections at TMP of 22 bar, acidic pH

Ion	Desal-5DK rejection (%)	Desal-5DL rejection (%)
Na^+	20	27
Ni^{2+}	>95	70
Co^{2+}	95	83

Co^{2+}, but it is only slightly more rejected by Desal-5DK membrane.

4.2.2. Acidic pH

Ionic rejections simulations were done to compare experimental results from an acidic multi-electrolyte solution to those predicted using fitted X_m and L_{eff} from a natural pH $NaNO_3$ solution. Results are presented in Fig. 5.

Predicted ionic rejections were not in good agreement with experimental results as reflected by higher values of standard deviation (5.8%). Only at elevated values of J_v for the Desal-5DK membrane the calculated rejections are close to experimental ones. Using X_m and L_{eff} fitted from an acidic $NaNO_3$ solution would not only improve simulation quality, but it would also increase the difficulty in obtaining the salt concentration as the use of the conductivity meter would not be possible.

For both membranes, experimental ionic rejections were higher at acid pH values than at the natural one. Monovalent ions rejections are close to 20% on Desal-5DK and almost 30% on Desal-5DL. Divalent ions are more rejected by Desal-5DK membrane (Table 5).

Despite the high heavy metal rejections (95% of Ni^{2+}), an acidic permeate solution would prevent the complexation part of the EC to happen. So filtrations at natural pH will be preferred.

5. Conclusion

The results of nanofiltration experiments showed that this technique could be efficiently applied as a pretreatment step in order to remove Ni^{2+} and Co^{2+} ions from a multi-electrolyte solution charged in $NaNO_3$. Suitable experimental conditions were determined prior to nanofiltration experiences by calculating solution speciation and evaluating simulated ionic rejections as a function of pH. In such conditions, the IEP of the two membranes could not be located but $CoCO_3$ precipitation is expected to occur for pH values higher than 7.

Ionic rejections were conveniently simulated by the use of effective membrane thickness and effective membrane charge obtained from the fit of experimental ionic rejections for a single salt $NaNO_3$ solution when the simulated solution had a natural pH. Simulations for the acidic ionic rejections were not in a good agreement with experimental results.

References

[1] L.K. Wang, Implementation of industrial ecology for industrial hazardous waste management, in: L.K. Wang, Y. Hung, H.H. Lo, C. Yapijakis (Eds.), Waste Treatment in the Process Industries, CRC/Taylor & Francis, Boca Raton, FL, (2005) 1–13.
[2] T.A. Kurniawan, G.Y.S. Chan, W.-H. Lo, S. Babel, Physico-chemical treatment techniques for wastewater laden with heavy metals, Chem. Eng. J. 118(1–2) (2006) 83–98.
[3] X.T. Le, P. Viel, P. Jégou, A. Sorin, S. Palacin, Electrochemical-switchable polymer film: An emerging technique for treatment of metallic ion aqueous waste, Sep. Purif. Technol. 69(2) (2009) 135–140.
[4] X. Lefebvre, J. Palmeri, Nanofiltration theory: Good co-ion exclusion approximation for single salts, J. Phys. Chem. B 109 (12) (2005) 5525–5540.
[5] A. Szymczyk, N. Fatin-Rouge, P. Fievet, C. Ramseyer, A. Vidonne, Identification of dielectric effects in nanofiltration of metallic salts, J. Membr. Sci. 287(1) (2007) 102–110.
[6] X. Lefebvre, J. Palmeri, P. David, Nanofiltration theory: An analytic approach for single salts, J. Phys. Chem. B 108(43) (2004) 16811–16824.
[7] J. Palmeri, N.B. Amar, H. Saidani, A. Deratani, Process modeling of brackish and seawater nanofiltration, Desalin. Water Treat. 9(1–3) (2009) 263–271.
[8] J. Palmeri, J. Sandeaux, R. Sandeaux, X. Lefebvre, P. David, C. Guizard, P. Amblard, J.F. Diaz, B. Lamaze, Modeling of multi-electrolyte transport in charged ceramic and organic nanofilters using the computer simulation program nanoFlux, Desalination 147(1–3) (2002) 231–236.
[9] A.E. Yaroshchuk, Dielectric exclusion of ions from membranes, Adv. Colloid Interface Sci. 85(2–3) (2000) 193–230.
[10] Y. Lanteri, P. Fievet, A. Szymczyk, Evaluation of the steric, electric, and dielectric exclusion model on the basis of salt rejection rate and membrane potential measurements, J. Colloid Interface Sci. 331(1) (2009) 148–155.
[11] A. Szymczyk, P. Fievet, Investigating transport properties of nanofiltration membranes by means of a steric, electric and dielectric exclusion model, J. Membr. Sci. 252(1–2) (2005) 77–88.
[12] J. Schaep, C. Vandecasteele, A.W. Mohammad, W.R. Bowen, Modelling the retention of ionic components for different nanofiltration membranes, Sep. Purif. Technol. 22–3(1–3) (2001) 169–179.
[13] A. Szymczyk, P. Fievet, S. Bandini, On the amphoteric behavior of Desal DK nanofiltration membranes at low salt concentrations, J. Membr. Sci. 355(1–2) (2010) 60–68.
[14] P. Wang, A. Anderko, Computation of dielectric constants of solvent mixtures and electrolyte solutions, Fluid Phase Equilib. 186(1–2) (2001) 103–122.
[15] J. Benavente, V. Silva, P. Pradanos, L. Palacio, A. Hernandez, G. Jonson, Comparison of the volume charge density of nanofiltration membranes obtained from retention and conductivity experiments, Langmuir 26(14) (2010) 11841–11849.

Appendix

ENP equation is given by Palmeri et al. [7]:

$$J_i = -\overline{D}_i \frac{\partial \overline{c}_i}{\partial x} - \frac{z_i \overline{c}_i \overline{D}_i}{RT} F \frac{\partial \Psi}{\partial x} + K_{i,c} \overline{c_i} \cdot J_v \quad (3)$$

In Eq. (3):

- J_i: molar ionic flux density (mol.m^{-2}s^{-1});
- $\overline{D_i}$: effective ionic diffusion coefficient in the membrane (m^2 .s^{-1});
- $\overline{c_i}(x)$: local average ionic concentration in the membrane (mol m^{-3});
- Ψ(x): local average electrical potential in the membrane (V);
- J_v: transmembrane solution volume flux density (L h^{-1} m^{-2});
- X: transverse distance across the membrane (m) ($0 \leqslant x \leqslant l_m$, where l_m is the membrane thickness).

As stated by Eq. (3), ionic flux is composed by diffusion, electrical migration, and convection terms. Effective ionic diffusion ($\overline{D_i}$) can be related to bulk solution ionic diffusion (D_i) by adding a hindered diffusion coefficient (K_i^d), membrane's tortuosity ,(τ) and porosity (φ): $\overline{D_i} = D_i \cdot K_i^d(\frac{\varphi}{\tau})$.

The volume-averaged Stokes equation is given by:

$$\frac{1}{L_p^0} J_v = -\frac{\partial P}{\partial x} - \rho \frac{\partial \Psi}{\partial x} \quad (4)$$

In Eq. (4):

- L_p^0: pure water hydraulic permeability (L/(h m^2 bar));
- $P(x)$: local average pressure in the membrane (bar);
- $\rho(x)$: local ionic charge density $\left(\rho(x) = \sum_i z_i \overline{C_i}(x)\right)$.

Resolution of Eqs. (3) and (4) are made by a series of assumptions always valuable to nanofiltration:

- Electroneutrality at the membrane, permeate, and feed is respected. This results in the following Eq. (5):
  $\sum_{i=1}^{n} z_i \overline{c_i}(x) + X_m = 0$ (for the membrane),
  $\sum_{i=1}^{n} z_i c_i^f(x) = 0$ (for the feed solution),
  $\sum_{i=1}^{n} z_i c_i^p(x) = 0$ (for the permeate).
- There is no electric current density (J_c) across the membrane $j_c = F \sum_i z_i J_i = 0$.
- Ionic concentration in the permeate is a function of both ionic and solvent fluxes $c_i^p = j_i / j_v$.

As stated in Section 3, dielectric exclusion is considered in the EHET theory by means of a partition coefficient ($k_{i,\text{dielectric}}$) calculated as follows:

$$k_{i,\text{dielectric}} = \exp(-\Delta W_{i,\text{Born}}) \exp(-\Delta W_{i,\text{im}}) \quad (5)$$

Born effect ($\Delta W_{i,\text{Born}}$) is due to an excess solvation energy caused by differences in the dielectric constant of the bulk solution and inside the pore. Such an effect is calculated by:

$$\Delta W_{i,\text{Born}} = \frac{z_i^2 e^2}{8\pi\varepsilon_0 k_B T r_i} \left(\frac{1}{\varepsilon_p} - \frac{1}{\varepsilon_b}\right) \quad (6)$$

In Eq. (7), instead of $r_{i,\text{cav}}$—the ionic cavity radius—as proposed by reference [11], the Pauling radius was used in our calculations. Dielectric constant of the bulk solution (ε_b) was considered to be 78.5 [14]. Dielectric constant of the solution inside the pores of the membrane (ε_p) was calculated by [15]:

$$\varepsilon_p = 5/8 \varepsilon_B \quad (7)$$

Image charge effects ($\Delta W_{i,\text{im}}$), not considered in the modified EHET theory used in this work, are caused by the interaction between an ion inside the pore of the membrane and a charge created by the ion itself at the pore/solvent interface [11]:

$$\Delta W_{i,\text{im}} = -\alpha_i \ln\left[1 - \left(\frac{\varepsilon_p - \varepsilon_m}{\varepsilon_p + \varepsilon_m}\right) \exp(-2\mu)\right] \quad (8)$$

With

- $\alpha_i = \dfrac{(z_i F)^2}{8\pi\varepsilon_0 \varepsilon_p RTN_A r_p}$ (9)

- $\mu = \kappa^b r_p \times \sqrt{\sum_i \dfrac{z_i^2 c_i^b \phi_i (\gamma_i^b / \gamma_i^m) \exp(-z_i \Psi_D - \Delta W_{i,\text{im}} - \Delta W_{i,\text{Born}})}{2I}}$ (10)

- $\kappa^b = \left(\dfrac{\varepsilon_0 \varepsilon_b RT}{2F^2 I^b}\right)^{-1/2}$ (11)

In Eqs. (7)–(12):

- e: elementary electron charge (1.60×10^{-19} coulombs);
- k_B: Boltzmann constant (1.38×10^{-23} m^2 kg s^{-2} K^{-1}),
- T: absolute temperature (K),
- ε_m: Membrane dielectric constant,
- F: Faraday constant (96,485.34 s A mol^{-1}),

R: ideal gas constant ($8.31\,\mathrm{J.mol^{-1}\,K^{-1}}$),
N_A: Avogadro constant ($6.02 \times 1.0^{23}\,\mathrm{mol^{-1}}$),
ϕ_i: steric exclusion partition coefficient ($k_{i,\mathrm{steric}}$),
$\gamma_i^{(b)(m)}$: bulk$^{(b)}$, membrane$^{(m)}$ activity coefficient,
I^b: bulk solution ionic force ($I^b = 1/2 \sum_i z_i^2 c_i^b$).